Available online at www.sciencedirect.com
ScienceDirect
Catalysis Today 118 (2006) 151–157
CATALYSIS TODAY
www.elsevier.com/locate/cattod

Oxygen diffusion in nanostructured perovskites

I.L. Zhogin [a,*], A.P. Nemudry [a], P.V. Glyanenko [a], Yu.M. Kamenetsky [a], H.J.M. Bouwmeester [b], Z.R. Ismagilov [c]

[a] *Institute of Solid State Chemistry and Mechanochemistry, 630128 Novosibirsk, Russia*
[b] *Institute for Nanotechnology, University of Twente, The Netherlands*
[c] *Institute of Catalysis, 630090 Novosibirsk, Russia*

Available online 31 July 2006

Abstract

Nonstoichiometric perovskite-related oxides (e.g. ferrites and cobaltites, etc.) are characterized by fast oxygen transport at ambient temperatures, which relates to the microstructural texturing of these materials, consisting wholly of nanoscale microdomains.

We have developed a heterogeneous diffusion model to describe the kinetics of oxygen incorporation into nanostructured oxides. Nanodomain boundaries are assumed to be the high diffusivity paths for oxygen transport whereas diffusion into the ordered domains proceeds much slower. The model has been applied for qualitative evaluation of oxygen diffusion parameters from the data on wet electrochemical oxidation of nanostructured perovskite $SrCo_{0.5}Fe_{0.2}Ta_{0.3}O_{3-y}$ samples.

Using Laplace transform methods, an exact solution is found for a ramped step-wise potential, allowing fitting of the experimental data to theoretical curves (in Laplace transforms). A further model generalization is considered by introducing additional parameters for the size distribution of domains and particles.
© 2006 Elsevier B.V. All rights reserved.

Keywords: Heterogeneous oxygen diffusion; Nanostructured perovskites; Electrochemical oxidation

1. Introduction

Mixed ionic electronic conducting (MIEC) oxides, in particular perovskite related materials, possessing high oxygen mobility, are of interest for applications such as SOFC electrodes, sensors and membranes for oxygen separation and partial oxidation of hydrocarbons in catalytic membrane reactors [1]. It is evident that the basic knowledge on the mechanism of oxygen transport in perovskites is necessary for the development of these devices and for modelling of their functioning.

In order to describe oxygen transport properties usually homogeneous diffusion of oxygen ions through random distributed vacancies is suggested [1]. It should be mentioned, however, that MIEC perovskite-related oxides are grossly nonstoichiometric and doped materials which can be considered as homogeneous solid solutions with a high concentration of structural defects (oxygen vacancies, dopant ions, etc.) only at temperatures higher then point of order-disorder transition ($T > T_t$). At $T < T_t$ structural ordering is observed in these materials, either a total one with the formation of superstructures where the defects are assimilated as structural elements, or a partial one with the formation of stoichiometric microdomains separated by disordered interfaces (domain boundaries, extended defects, etc.). In the latter case, defects, e.g. oxygen vacancies, are redistributed inhomogeneously along the material: some of them are ordered inside the microdomains as structural elements, whereas the rest of the overstoichiometric defects are ejected to the vicinity of the interfaces where they have higher mobility. Such a situation has been described in the microdomain concept by J.C. Anderson [2] and was confirmed experimentally in the works of M.Á. Alario-Franco, J.-C. Grenier and P. Hagenmuller [3–5]; unmixing of nonstoichiometric and doped oxides with perovskite-related structures at $T < T_t$ results in the formation of coherently stacked microdomains of 5–50 nm in size and mobile oxygen ions situated in the vicinity of the microdomain boundaries.

Another reason for the intrinsic inhomogeneity of non-stoichiometric and doped MIEC perovskites relates to a strong tendency toward phase separation in systems with strongly

* Corresponding author. Tel.: +7 383 3394298.
E-mail addresses: zhogin@inp.nsk.su (I.L. Zhogin), nemudry@solid.nsk.su (A.P. Nemudry).

0920-5861/$ – see front matter © 2006 Elsevier B.V. All rights reserved.
doi:10.1016/j.cattod.2006.02.088

Nomenclature

$U(t)$	voltage pulse between the sample and reference electrodes (V)
t_0	time of linear growth of voltage pulse (s)
h	dimensionless parameter of the (step in) voltage pulse
$J(t)$	current passing through the electrochemical cell (A)
t	time measured after start of the voltage pulse (s)
p	parameter of Laplace transform (1/s)
$\hat{U}(p)$, $\hat{J}(p)$	Laplace transforms
$Q = \hat{J}(0)$	total charge serving as normalizing factor (C)
x	radial coordinate in a sphere (m)
R	radius of sample particles (m)
r	radius of nanodomains ($R \gg r$)
n_d	concentration of nanodomains (1/m^3)
v_1, v_2	volume fractions occupied by nanodomains and interfaces ($v_1 = 4\pi r^3 n_d/3, v_2 = 1 - v_1$)
D_1	coefficient of slow diffusion in nanodomain (m^2/s)
D_2	effective fast diffusivity (due to interfaces)
c_1, c_2	oxygen concentration in nanodomains and interfaces, respectively
$c_1 = \gamma c_2$	condition at boundary between nanodomain and interface (inter-domain region)
$\tau_1 = r^2/D_1$	first diffusion time (s)
$\tau_2 = R^2/D_2$	second diffusion time (for "fast" diffusion)
$\alpha = \gamma v_1/v_2$	dimensionless parameter of the model (α, τ_1, τ_2 form full set of fitting parameters)
$\kappa = \sqrt{p/D}$	useful parameter to write current transform (1/m)
$F(y)$, $f(y)$	functions of dimensionless argument used to write solution to the model of heterogeneous diffusion [$y = p\tau$, $f(y) = F(\sqrt{y})$]
$n = QM/mF$	charge transfer (e$^-$/formulae unit); here M is molecular weight of the sample, m weight of the sample, F Faraday constant
$n/2$	a number of intercalated oxygen ions per formulae unit
T_t	order-disorder transition temperature

correlated electrons. Electron conducting oxides with transition metals having different charges (for example, $Mn^{3/4+}$, $Co^{3/4+}$, $Cu^{2/3+}$, etc.) and magnetic states can break into a stable state made of nanoscale coexisting clusters because of complicated electron-phonon and magnetic interactions [6].

So, at $T < T_t$ MIEC oxides can be considered as nanostructured materials which are known to be able to show enhanced ionic transport properties owing to the high density of disordered interfaces [7]. In order to develop an adequate mathematical model describing oxygen transport at $T < T_t$, it is necessary to take into account heterogeneous character of oxygen diffusion in nanostructured perovskites.

Previously, as reported by Goldberg et al. [8,9], one of us proposed a model for oxygen diffusion in microdomain textured perovskites in which the domain boundaries are high diffusivity paths and changes in the oxygen stoichiometry in domains occurs due to a two-phase reaction. In the present work we continue modeling the oxygen transport in nanostructured materials having the channels for enhanced oxygen diffusion, however, unlike the previous papers, here we assume that oxidation of microdomains occurs as a result of one-phase reaction. To describe oxygen transport in such a system, we generalized the model of heterogeneous diffusion proposed by Bokshtein et al. [10] for description of diffusion processes in polycrystalline metals.

Since MIEC perovskites exhibit fast oxygen transport even at room temperature [11], the model was applied for the evaluation of oxygen diffusion parameters from the data on wet electrochemical oxidation of nanostructured perovskite $SrCo_{0.5}Fe_{0.2}Ta_{0.3}O_{3-y}$ samples in 1 M KOH at ambient temperatures. The choice of the material is because $SrCo_{0.5}Fe_{0.2}Ta_{0.3}O_{3-y}$ samples possess high oxygen transport properties and enhanced chemical stability in reducing environments and can be considered as promising membrane materials for partial oxidation of hydrocarbons [12].

Thus, the objectives of this work are: (1) the development of a mathematical model describing oxygen transport in nanostructured oxides in which the domain boundaries are the channels for enhanced oxygen diffusion, whereas oxygen penetration into domains occurs as a result of one-phase reaction; (2) its adaptation for the analysis of current transients under electrochemical oxidation of nanostructured materials; and (3) experimental verification with the samples of practical interest.

2. Experimental

The samples of $SrCo_{0.5}Fe_{0.2}Ta_{0.3}O_{3-y}$ nonstoichiometric perovskite were synthesized by solid-state reaction from the corresponding metal oxides and carbonates with preliminary homogenization of the starting materials in a planetary ball mill. A stoichiometric mixture of the powders was calcined at 900 °C, pressed in pellets, annealed in air at 1400 °C for 6 h and cooled in the furnace. Different oxygen stoichiometry of materials was achieved by (a) slow cooling in the furnace, (b) annealing at 950 °C in a quartz ampoule under dynamic vacuum ($P \sim 10^3$ Pa) and quenching of the sample in the ampoule to room temperature in water.

Phase analysis was performed by means of X-ray diffraction with DRON 3, whereas the oxygen content was determined by iodometric titration and thermogravimetry. Electron microscopy was applied for microstructural studies.

Electrochemical experiments were performed at room temperature by means of potentiostat/galvanostat PI-50-1 (three-electrode cell, 1 M KOH electrolyte, Hg/HgO reference electrode) with working electrodes of $SrCo_{0.5}Fe_{0.2}Ta_{0.3}O_{3-y}$ polycrystalline material (17–18 mg) pressed into Pt grids along with 1 wt.% of Teflon and 15–20 wt.% of acetylene black.

Chronopotentiometric investigation of the anode oxidation of $SrCo_{0.5}Fe_{0.2}Ta_{0.3}O_{3-y}$ in the galvanostatic mode combined with in situ X-ray diffraction was carried out to study the mechanism of phase transformations under the changes in the oxygen stoichiometry of the samples. For the kinetics studies (potentiostatic mode) the working electrode was placed in a cell at 25 °C and was maintained up to equilibrium potential U_0. At $t = 0$ a voltage pulse between the working electrode and reference electrode is applied. Re-equilibration through diffusion of oxygen into the working electrode material takes place. The rate of re-equilibration can be measured easily by monitoring the electric current passing through the cell. A more detailed description of electrochemical techniques can be found in refs. [13,14,11].

3. Theoretical model

Similar to the model of spheres filling a half-space (grains in a thick metal plate, see [10]), we consider a model in which the small spheres are inside large ones (nanodomains inside the perovskite powder particles). The simple geometry of our model allows us to derive an exact solution for the current passing through the cell using the Laplace transform method.

The inverse Laplace transformation to determine the original function is not possible in the analytical form (in analytical functions; this is the reason why one usually analyzes only the asymptotic current behavior at short and long times) [14]. Though there are computational methods to do the inverse Laplace transformations [15], they require intensive calculations (double Fourier transforms). Therefore, we have chosen another way to compare our experiment with the model. After we perform numerical Laplace transformation of the measured current function, $J_{exp}(t)$, (as well as potential function, if it is measured and is not given "analytically" with potentiostate) we adjust the experimental transform, $\hat{J}_{exp}(p)$, with model curves $\hat{J}_{th}(p)$ (which depend on the applied potential profile).

However, computer inversion of the Laplace transform may be useful for verifying the best approximation, or for the better choosing among several minima, if they occur.

A two-level model of spheres is used to describe the current passing through an electrochemical cell under potential of a chosen profile.

3.1. Diffusion in a spherical particle

The diffusion equation for a spherical particle, when the space derivatives (Laplacian) are reduced to differentiation over the radius, is written as follows:

$$\frac{\partial(x\,c)}{\partial t} = D\frac{\partial^2(x\,c)}{\partial x^2}. \tag{1}$$

here $c(t, x)$ is the concentration of the diffusing species, R the particle radius, and x the radial coordinate, $0 \le x \le R$. For initial and boundary conditions we have

$$c(t<0,x) = 0, \qquad c(t, x = R) = c_R(t).$$

Using the Laplace transform of $c(t, x)$

$$\hat{c}(p,x) \equiv \int_0^\infty c(t,x)e^{-pt}\,\mathrm{d}t$$

turns partial derivatives (1) into an ordinary differential equation

$$\frac{\partial^2(x\hat{c})}{\partial x^2} = \frac{p}{D}x\hat{c}. \tag{2}$$

Applying a boundary condition, $\hat{c}(p, R) = \hat{c}_R(p)$, one can easily find the exact solution to Eq. (2),

$$\hat{c}(p,x) = \hat{c}_R(p)\frac{\kappa R}{\sinh(\kappa R)}\frac{\sinh(\kappa x)}{\kappa x}, \quad \kappa = \sqrt{p/D}. \tag{3}$$

Diffusion current (and electric one, if diffusing component carriers charge q), passing through the whole particle boundary, may be expressed as follows:

$$J(t) = 4\pi q\int_0^R \frac{\partial c(t,x)}{\partial t}x^2\,\mathrm{d}x,$$

$$\hat{J}(p) = 4\pi q\frac{p\hat{c}_R(p)R}{\sinh(\kappa R)}\int_0^R \sinh(\kappa x)x\,\mathrm{d}x. \tag{4}$$

One may expect that the diffusion coefficient to be independent of the concentration, provided that the oxygen content in the perovskite lattice changes only slightly, e.g. $\Delta y < 0.1$. For this purpose the amplitude of potential pulse, U_A, applied to the cell, should be small enough. We assume that the access of oxygen ions to the particles is not limited and, hence, there is a linear dependence between concentration and the potential

$$\frac{c_R(t)}{c_A} = \frac{U(t)}{U_A}.$$

In our experiments we used the potential steps of the following form (see Fig. 6a):

$$\frac{U(t)}{U_A} = \begin{cases} 0, & t<0 \\ h+(1-h)t/t_0, & 0 \le t \le t_0; \\ 1, & t > t_0 \end{cases}$$

this gives the Laplace transform ($0 \le h \le 1$):

$$\frac{p\hat{c}_R(p)}{c_A} = h + (1-h)\frac{1-e^{-pt_0}}{pt_0}\left(\overset{p\to 0}{\longrightarrow}1\right). \tag{5}$$

Introducing the value $Q = \hat{J}(0) = 4\pi R^3 q c_A/3$ for a total charge passed through the cell, and using Eqs. (3)–(5) we obtain ($\tau = R^2/D$ is a characteristic diffusion time for a sphere of radius R; $\sqrt{p\tau} = \kappa R$)

$$\frac{\hat{J}(p)}{Q} = \frac{p\hat{c}_R(p)}{c_A}F(\sqrt{p\tau}), \tag{6}$$

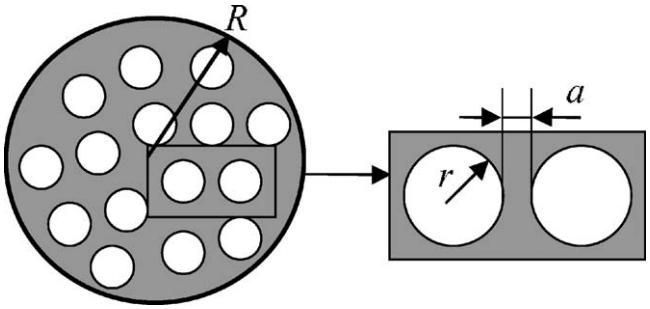

Fig. 1. Regions of slow (white) and fast (grey) diffusion.

where

$$F(y) \equiv \frac{3\coth(y)}{y} - \frac{3}{y^2}\left(\overset{y\to 0}{\longrightarrow} 1 - \frac{y^2}{15} + \cdots\right). \tag{7}$$

3.2. Heterogeneous diffusion model: spheres of two types

Let us imagine that the particles in the sample are heterogeneous (see Fig. 1) and contain domains of a typical size r, where the diffusion rate is small, D_1, and interfaces (regions neighboring with domains boundaries), where the diffusion rate is high, D_2. More exactly, let us consider D_2 as an effective diffusion coefficient for a porous particle, obtained, when all domains are removed, as if they are non-permeable for diffusion, i.e. $D_1 = 0$. This effective coefficient may change not only with temperature, but also with parameters related to the nanodomain structure, such as oxygen content, quenching rate, etc.

If diffusion coefficient D_1 is small but not equal to zero, then the diffusion equation should reflect oxygen incorporation inside the domains. One may assume that the concentration along the boundary of each domain is approximately the same (since transport to the boundary is fast) and proportional to the current local concentration:

$$c_{1r}(t) = \gamma c_2(x,t).$$

Therefore, we may write an effective diffusion equation in a heterogeneous particle instead of Eq. (1):

$$qv_2\left(\frac{\partial c_2}{\partial t} - D_2\frac{\partial^2(xc_2)}{x\partial x^2}\right) = -n_{\mathrm{d}}J_1(t,x).$$

Here n_{d} is the concentration of domains, J_1/q the diffusion current into domains, $v_1 = 4\pi r^3 n_{\mathrm{d}}/3$, $v_2 = 1 - v_1$ are volume fractions for regions of slow and fast diffusion, respectively. After the Laplace transformation we obtain (taking into account Eqs. (5) and (6)):

$$\frac{\partial^2(x\hat{c}_2)}{\partial x^2} = \frac{p}{D_2}x\hat{c}_2(1 + \alpha F(\sqrt{p\tau_1})), \tag{8}$$

where $\alpha = \gamma v_1/v_2$ is proportional to the ratio of above mentioned volume fractions (see Fig. 1).

As was mentioned in [10], the equilibrium concentrations (of diffusant) along the boundaries and inside the domains (i.e. grains in [10]) may not coincide. Therefore, the dimensionless parameter α may include not only geometry but also the concentration factor γ.

One may derive the final expression for the current using Eq. (8) (it is necessary to remember that the particle is heterogeneous):

$$\hat{J}(p) = 4\pi R^2 D_2 \left.\frac{\partial\hat{c}_2}{\partial x}\right|_{x=R} = Q\frac{p\hat{c}_{2R}(p)}{c_A} \times \frac{1+\alpha f(p\tau_1)}{1+\alpha} f(p\tau_2[1+\alpha f(p\tau_1)]). \tag{9}$$

Here notations $f(y) \equiv F(\sqrt{y})$, $\tau_1 \equiv r^2/D_1$, $\tau_2 \equiv R^2/D_2$ (see Eqs. (5)–(7)) are introduced.

3.3. Assembly of particles, particle size distribution

If powder particles are of different sizes, then the current expression (6) and expression (9) should be integrated with the function of volume (mass) distribution of particles, $M(R)$ (norm per unit):

$$\frac{\hat{J}(p)}{Q} = \frac{p\hat{c}_R(p)}{c_A}\int_0^\infty F(\kappa R)M(R)\,\mathrm{d}R.$$

If the 'relative' dispersion of the distribution,

$$\Delta_R = \frac{\langle(R-R_0)^2\rangle}{R_0^2}\,(R_0 = \langle R\rangle),$$

is small, we retain only the first correction term, changing functions in (9) or (6) as follows (prime means differentiation by argument):

$$F(\kappa R) \to F^*(\kappa R_0) = F(\kappa R_0) + \frac{1}{2}\kappa^2 R_0^2 F''(\kappa R_0)\Delta_R, \tag{10}$$

where

$$y^2F''(y) = 6\left(1 + \frac{y^2}{\sinh^2 y}\right)\left(1 + \frac{y}{\tanh y}\right) - \frac{24}{y^2}.$$

One may obtain this correction by e.g. integration with formal distribution (delta functions):

$$M(R) = \delta(R-R_0) + \frac{1}{2}\delta''(R-R_0)\Delta_R R_0^2,$$

which has proper first two moments. Saddle-point integration with the Gaussian distribution $M(R) \propto \exp(-(R/R_0-1)^2/2\Delta_R)$ gives the same result.

In a similar manner one may correct for the size dispersion of nanodomains, Δ_r, and dispersion of parameter α, Δ_α, as well.

4. Experimental results and computation

According to the X-ray diffraction data, $SrCo_{0.5}Fe_{0.2}Ta_{0.3}O_{3-y}$ samples obtained either by slow cooling or by quenching in vacuum are single-phase and have cubic perovskite structure

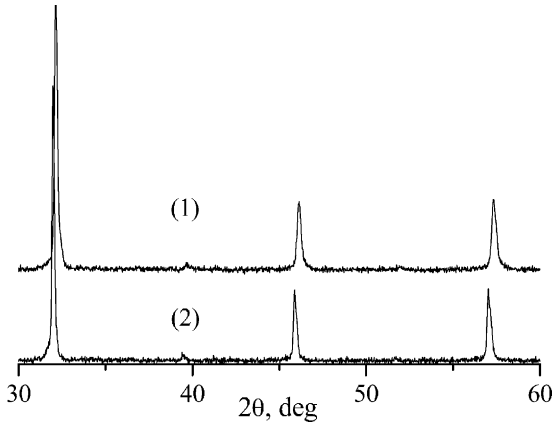

Fig. 2. Diffraction patterns of samples $SrCo_{0.5}Fe_{0.2}Ta_{0.3}O_{3-y}$: (1) as prepared, (2) after annealing in vacuum ($P \sim 10^3$ Pa) at 950 °C and quenching.

with the parameters 3.934 Å and 3.952 Å, respectively (Fig. 2). Iodometric titration showed that quenching of the samples in vacuum causes a decrease in oxygen content $(3 - y)$ from 2.92 to 2.70.

In spite of the fact that XRD suggests single-phase behavior, the HREM data show that the quenched samples possess a nanodomain texture (Fig. 3) with a typical domain size of about 10 nm. Such a situation is typical for the nanostructured materials with coherent/semicoherent stacking of domains: in terms of X-ray diffraction they behave as homogeneous single phases [2–5].

In order to determine the mechanism of oxidation of the nanostructured $SrCo_{0.5}Fe_{0.2}Ta_{0.3}O_{3-y}$ perovskite, we carried out chronopotentiometric measurements of the electrochemical anodic oxidation of the samples in the galvanostatic mode, combined with in situ X-ray diffraction studies. Measurements of the potential of the working (sample) electrode versus the charge that passed through the electrochemical cell ($n = JtM/mF$), which is connected through a simple relation with the amount of inserted oxygen $x = n/2$, provide evidence of phase transitions in the oxide under the changes of the oxygen stoichiometry. The character of phase transitions can be judged

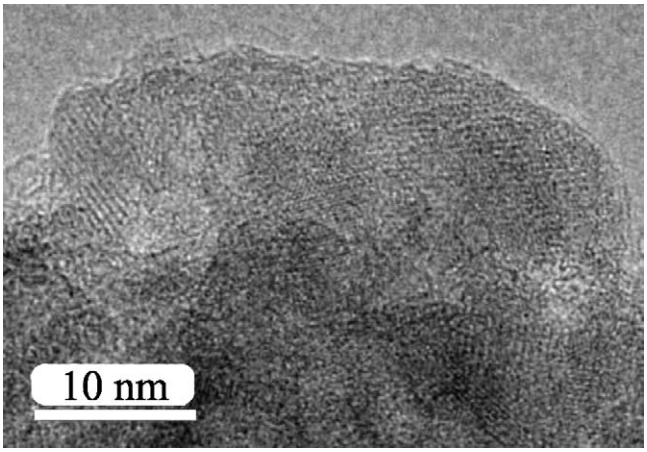

Fig. 3. High resolution image of $SrCo_{0.5}Fe_{0.2}Ta_{0.3}O_{2.7}$ sample possessing nanodomain texture.

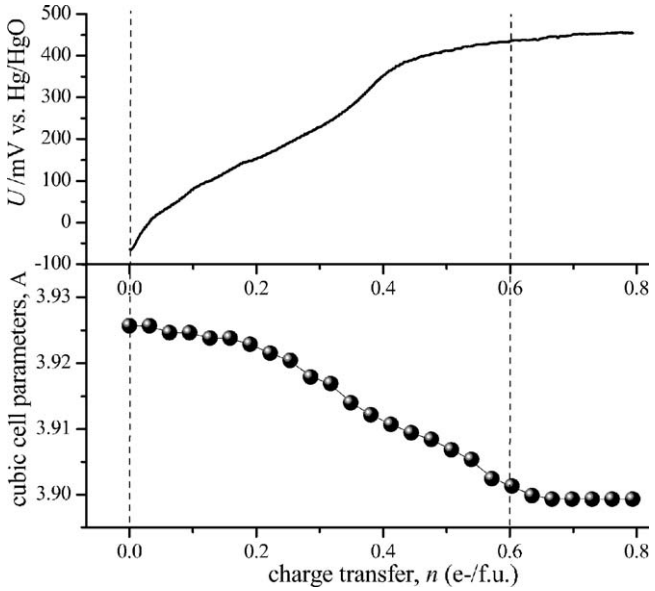

Fig. 4. In situ anodic oxidation of $SrCo_{0.5}Fe_{0.2}Ta_{0.3}O_{2.7+x}$: (a) potential U vs. charge transfer n, (b) change of unit-cell parameters with n, $n/2 = x$.

about from the shape of U—n curve and in situ X-ray diffraction data. Fig. 4 shows the results of chronopotentiometry and evaluation of the in situ XRD data.

Monotonous changes in the unit cell parameters and potential versus charge transfer provide evidence of one-phase mechanism of oxidation [11,16].

For kinetic studies, we used the powdered samples with particle size distribution shown in Fig. 5.

So, in the course of preliminary studies nanostructured $SrCo_{0.5}Fe_{0.2}Ta_{0.3}O_{2.7}$ perovskite samples were obtained, particle size distribution for powdered samples and the size of nanodomains were determined. It was shown that sample oxidation occurs as a result of one-phase reaction; the potential range within which the oxidation of the sample occurs was determined.

After that, kinetic studies of potentiostatic oxidation of $SrCo_{0.5}Fe_{0.2}Ta_{0.3}O_{2.7}$ perovskite were carried out according to

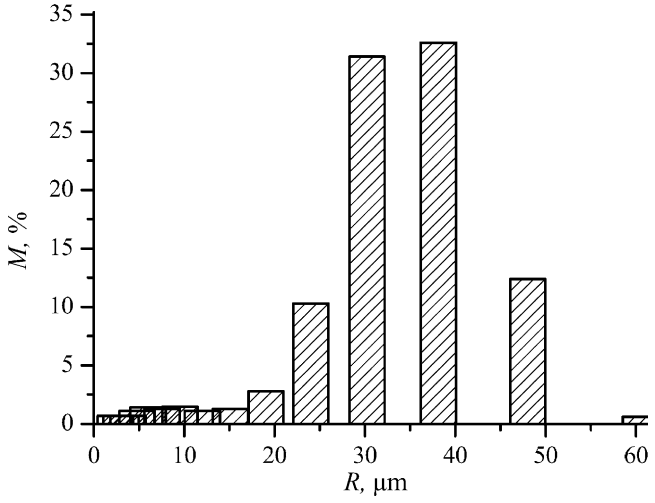

Fig. 5. Mass distribution of particles over size.

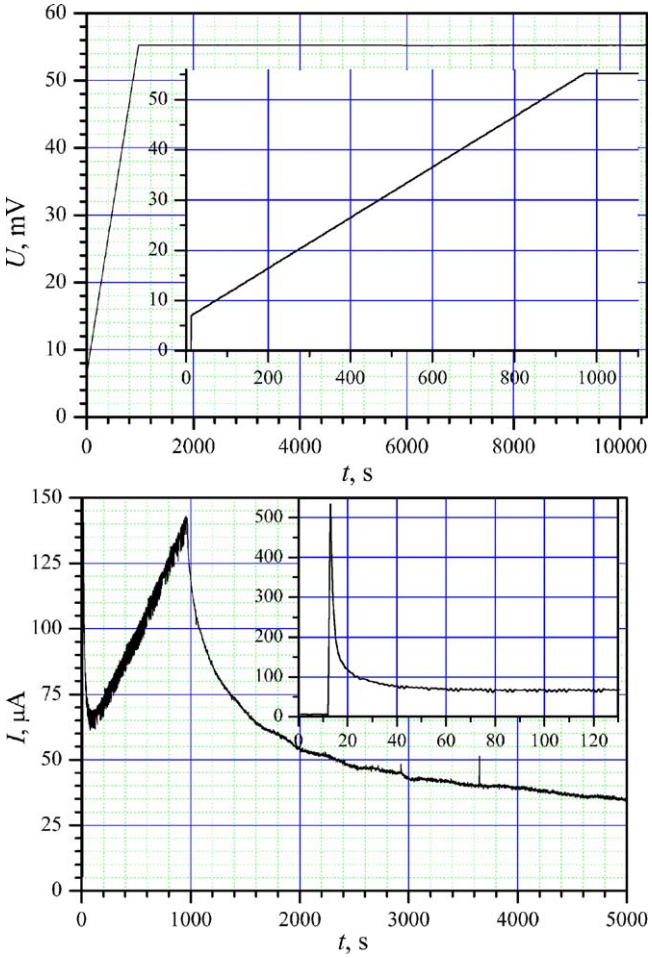

Fig. 6. Applied potential (a) and current transient (b) vs. time.

the procedure described in the Experimental section and in [11,13,14]; the analysis of current transients was also carried out (optimization of parameters τ_1, τ_2 and α) with the help of the Laplace transformation.

Fig. 6 shows $U(t)$ and $J_{exp}(t)$ functions versus time, obtained in one of experiments. The time of current measurement averaging was 1 s. This obstacle somewhat distorted the current plot at short times.

Computations were performed in MatLab. For the data, presented in Fig. 6, potential step parameters are the following (see Eqs. (5) and (9)):

$h = 7/55.25;\ t_0 = 958;\ \%t_0$ in seconds.

After $\hat{J}_{exp}(p)/Q$ was calculated (exponential slope at long times ($t > 3000$ s) was considered analytically), correction for the time of microammeter integration (1 s) was introduced:

$JeL = JeL. * p./(1 - \exp(-p));\ \%1$s.

Then optimization over three parameters entering the model function of current (Eq. (9)) was done.

Computing results are shown in Fig. 7, model parameters for theoretical curve (dotted line) being as follows:

$\tau_1 = 49$ s, $\tau_2 = 19 \times 10^3$ s, $\alpha = 4.8$.

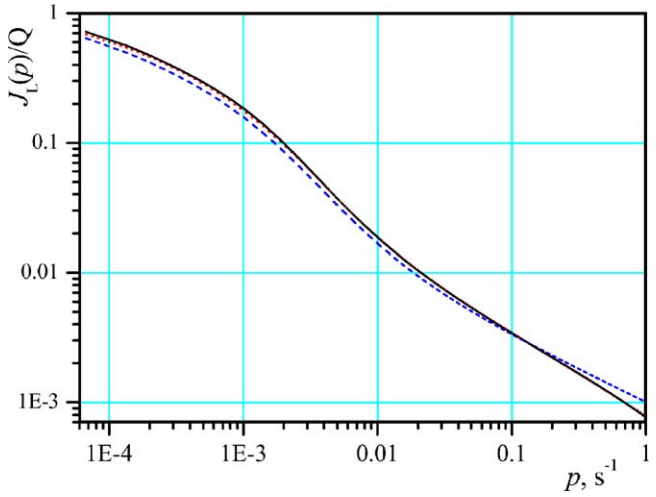

Fig. 7. Normalized Laplace transform of experimental data (solid; $Q = 0.44$ C) and fitting model curves for inhomogeneous (dot) and homogeneous (dash; $\alpha = 0$) model.

Using values $r \sim 10$ nm, $R = 32$ μm, one may estimate diffusion coefficients

$D_1 = 2 \times 10^{-13}$ cm^2/s, $D_2 = 5 \times 10^{-10}$cm^2/s.

Let us note that fitting by the homogeneous model gives essentially larger errors (see dashed curve in Fig. 7), and yields another value: $\tau_2 = 15 \times 10^4$ s.

5. Discussion and conclusions

In the present work we suggest a model describing oxygen transport in nanostructured materials having the channels for enhanced oxygen diffusion. Formally, we generalize the model of heterogeneous diffusion proposed by Bokshtein et al. [10] to describe diffusion processes in polycrystalline metals. Unlike the model of heterogeneous diffusion in which the grain spheres closely fill the semi-space, we consider another version of geometry: nanodomain spheres (r) form larger spheres which are the particles (radius R, $R \gg r$) of the oxide under investigation. So, the model proposed by Bokshtein et al. is a particular case of our model when the radius R tends to infinity. Changes in the geometry are due to the necessity of adapting of the model to the experimental conditions. For an express estimation of the oxygen transport properties of MIEC materials, we proposed using relatively simple techniques of wet electrochemistry. However, one should keep in mind that the model is valid within the temperature range ($T < T_t$) of existence of nanodomain texture. The question to what extent the wet electrochemical data correspond to the high-temperature data obtained under actual performance conditions is the subject of further investigations.

Using the Laplace method we have obtained an exact solution in transforms to our model. The inverse transition to the original is impossible in the analytical form; in such cases the consideration is usually limited to the analysis of the asymptotic behavior. Correspondingly, in the experiment one

analyzes either the initial region for short time or the region of long times (in comparison with the characteristic time of diffusion for this geometry) [13,14].

To analyze the electrochemical data (current transients), we realized a new approach allowing us to use the current transients as a whole: we carry out the numerical Laplace transform for the experimental current curve, then make the fitting procedure, compare the obtained transform with the analytical solutions of the model.

An important parameter of the model, along with the radius of domains r and radius of particles R, coefficients of fast (along domain boundaries, D_2) and slow diffusion (inside domains, D_1), is a dimensionless parameter α which has a sense of the ratio of fraction of inserted oxygen which finally (after equilibration) gets into the region of slow diffusion (domains) or into the region of fast diffusion (interfaces). According to our calculations, the part of new oxygen connected with highly conducting interfaces accounts for $100\%/(1 + \alpha) = 17\%$ of the all inserted oxygen.

With our developed model, we have shown that nanostructuring results in heterogeneous oxygen diffusion in domains and along the interfaces; the difference in diffusion coefficients may attain several orders of magnitude. The most important issue is that stationary flux of oxygen ions through nanostructured perovskite membranes at temperatures lower than the point of the order–disorder transition T_t is determined mostly by coefficient D_2. Since activation energy E_a, necessary for the oxygen ions migration along the domain boundaries (d.b.), may be essentially lower than that for the bulk (b.) diffusion, E_a(d.b.)$\sim$l/2 E_a(b.) [17], oxygen permeable membranes made of nanostructured oxides are able to provide several orders of magnitude higher oxygen fluxes at the working temperatures below the order–disorder transition point.

We shall further study the kinetics of nanostructured perovskites oxidation at various temperatures to determine the activation energy for oxygen ion migration along the interfaces and inside the domains and develop the method for measuring oxygen diffusion parameters in the nanostructured materials. Comparing the data obtained at low temperature by means of relatively simple wet electrochemical technique with the data related to oxygen permeability at high temperatures, we might define the mechanism of oxygen transport in nanodomain textured oxides, elucidate the factors determining the high values of oxygen fluxes in these materials and open the strategies to develop new oxygen-conducting materials operating at moderate temperature.

Acknowledgement

The work has been supported by RFBR-NWO (03-03-89005) and RFBR (05-03-32640, 05-03-08109) grants.

References

[1] H.J.M. Bouwmeester, A.J. Burggraaf, Dense ceramic membranes for oxygen separation, in: A.J. Burggraaf, L. Cot (Eds.), Fundamentals of Inorganic Membrane Science and Technology, Elsevier, Amsterdam, 1996, p. 435.
[2] J.S. Anderson, The thermodynamics and theory of nonstoichiometric compounds, in: A. Rabenau (Ed.), Problems of Nonstoichiometry, North-Holland Publ. Co., Amsterdam, 1970, p. 1.
[3] M.Á. Alario-Franco, J.M. Gonzalez-Calbet, M. Vallet-Regi, J.-C. Grenier, J. Solid State Chem. 49 (1983) 219.
[4] M. Vallet-Regi, J.M. Gonzalez-Calbet, J. Verde, M.Á. Alario-Franco, J. Solid State Chem. 57 (1985) 197.
[5] J.-C. Grenier, N. Ea, M. Pouchard, P. Hagenmuller, J. Solid State Chem. 58 (1985) 243.
[6] E. Dagotto, T. Hotta, A. Moreo, Phys. Rep. 344 (2001) 1–153.
[7] P. Heitjans, S. Indris, J. Phys.: Condens. Matter 15 (2003) R1257–R1289.
[8] E. Goldberg, A. Nemudry, V. Boldyrev, R. Schöllhorn, Solid State Ionics 110 (1998) 223.
[9] E. Goldberg, A. Nemudry, V. Boldyrev, R. Schöllhorn, Solid State Ionics 122 (1999) 17.
[10] B.S. Bokshtein, A.I. Magidson, I.L. Svetlov, Fizika Metallov i Metallovedenie 6 (1958) 1040, In Russian.
[11] A. Nemudry, E.L. Goldberg, M. Aguirre, M.Á. Alario-Franco, Solid State Sci. 4 (2002) 677.
[12] P. Glyanenko, A. Nemudry, Z.R. Ismagilov, H.J.M. Bouwmeester, Investigation of structure, phase transition and oxygen mobility in $SrCo_{0.8-x}Fe_{0.2}Ta_xO_{3-y}$ mixed conductors, 7-th ICCMR, 11–14 September 2005. Book of Abstracts, Cetraro, Italy, p. 241.
[13] S. Sunde, K. Nişancioğlu, T.M. Gür, J. Electrochem. Soc. 143 (11) (1996) 3497.
[14] C.J. Wen, C. Ho, B.A. Boukamp, I.D. Raistick, W. Weppner, R.A. Huggins, Int. Metals Rev. 5 (1981) 253.
[15] B. Hüpper, E. Pollak, A new method for numerical inversion of the Laplace transform, http://arXiv.org/physics/9807051.
[16] A. Nemudry, P. Rudolf, R. Schöllhorn, Chem. Mater. 8 (1996) 2232.
[17] P. Kofstad, High Temperature Corrosion, Elsevier, London, 1988, p. 558.